

Rearrangement of the antiferromagnetic ordering at high magnetic fields in SmFeAsO and SmFeAsO_{0.9}F_{0.1} single crystals

S. Weyeneth,¹ P. J. W. Moll,² R. Puzniak,³ K. Ninios,⁴ F. F. Balakirev,⁵ R. D. McDonald,⁵ H. B. Chan,⁴ N. D. Zhigadlo,² S. Katrych,² Z. Bukowski,² J. Karpinski,² H. Keller,¹ B. Batlogg,² and L. Balicas^{6,*}

¹Physik-Institut der Universität Zürich, Winterthurerstrasse 190, CH-8057 Zürich, Switzerland

²Laboratory for Solid State Physics, ETH Zurich, CH-8093 Zurich, Switzerland

³Institute of Physics, Polish Academy of Sciences, Aleja Lotników 32/46, PL-02-668 Warsaw, Poland

⁴Department of Physics, University of Florida, Gainesville, Florida 32611, USA

⁵National High Magnetic Field Laboratory, Los Alamos National Laboratory, Los Alamos, New Mexico 87545, USA

⁶National High Magnetic Field Laboratory, Florida State University, Tallahassee, Florida 32310, USA

The low-temperature antiferromagnetic state of the Sm-ions in both nonsuperconducting SmFeAsO and superconducting SmFeAsO_{0.9}F_{0.1} single crystals was studied by magnetic torque, magnetization, and magnetoresistance measurements in magnetic fields up to 60 T and temperatures down to 0.6 K. We uncover in both compounds a distinct rearrangement of the antiferromagnetically ordered Sm-moments near 35 – 40 T. This is seen in both, static and pulsed magnetic fields, as a sharp change in the sign of the magnetic torque, which is sensitive to the magnetic anisotropy and hence to the magnetic moment in the *ab*-plane, (*i.e.* the FeAs-layers), and as a jump in the magnetization for magnetic fields perpendicular to the conducting planes. This rearrangement of magnetic ordering in 35 – 40 T is essentially temperature independent and points towards a canted or a partially polarized magnetic state in high magnetic fields. However, the observed value for the saturation moment above this rearrangement, suggests that the complete suppression of the antiferromagnetism related to the Sm-moments would require fields in excess of 60 T. Such a large field value is particularly remarkable when compared to the relatively small Néel temperature $T_N \simeq 5$ K, suggesting very anisotropic magnetic exchange couplings. At the transition, magnetoresistivity measurements show a crossover from positive to negative field-dependence, indicating that the charge carriers in the FeAs planes are sensitive to the magnetic configuration of the rare-earth elements. This indicates a finite magnetic/electronic coupling between the SmO and the FeAs layers which are likely to mediate the exchange interactions leading to the long range antiferromagnetic order of the Sm ions.

PACS numbers: 74.25.-q, 74.25.Ha, 74.70.Xa, 75.30.Kz

I. INTRODUCTION

Soon after the discovery of high-temperature superconductivity in the cuprate system La_{2-x}Ba_xCuO₄,¹ a new class of superconducting compounds based on CuO₂ layers was found. Similarly, the recent discovery of superconductivity in LaFeAsO_{1-x}F_y, with a transition temperature $T_c \simeq 26$ K,² led to the discovery of a whole new class of iron-based superconductors REFeAsO_{1-x}F_y, where RE denotes a rare earth element, with T_c 's up to $\simeq 55$ K.³ Fe-based superconductors share some common properties with the cuprates such as a layered crystallographic structure, the presence of competing orders, low carrier density, a small coherence length, and possibly also an unconventional pairing mechanism. As in the cuprates, superconductivity sets in upon doping an antiferromagnetic parent compound.⁴ Nevertheless, there are some important differences: the Fe-based superconductors emerge by doping a metallic parent compound, the anisotropy is in general lower when compared to that of the cuprates, and the symmetry of the order parameter is claimed to be s_{\pm} -wave with Fermi-surface nesting playing a major role.⁵ Therefore, the fundamental question arises whether the mechanisms leading to superconductivity in both families of high temperature

superconductors share a common origin.

Neutron scattering experiments revealed that in the undoped compounds the magnetic moments of the Fe ions display a collinear antiferromagnetic order, which is claimed to be itinerant in character.⁶ It was suggested that the antiferromagnetism in undoped compounds is driven by a nesting instability,^{5,7} connecting cylindrical Fermi surfaces of hole and electron character through the antiferromagnetic modulation vector $\vec{Q} = (\pi, \pi)$ (in the original and undistorted tetragonal Brillouin zone),⁸ hence forming a spin-density wave. Interestingly, the doping dependent phase diagram for the different iron-based superconductors exhibit peculiar features with some compounds exhibiting either coexistence⁹ or competition¹⁰ of antiferromagnetism with superconductivity.

The replacement of La in LaFeAsO_{1-x}F_y by a magnetic rare earth element as *e.g.* Sm has remarkable consequences: It not only increases the value of T_c to 55 K,³ but also leads to antiferromagnetic ordering of the rare-earth moments at low temperatures,¹¹⁻¹⁸ coexisting in the underdoped compounds with the spin-density wave state due to the magnetic correlation of the Fe ions.^{12,17,18} At first glance one could expect that the incorporation of ions with a large magnetic moment such as

Sm (having a free ion moment of $\mu^{\text{Sm}} \simeq 0.84 \mu_{\text{B}}$)¹⁹ to be detrimental for any superconducting pairing scenario.²⁰ However, it has been argued that the main effect of rare-earth elements is related to their ionic radii, and that ions with different radii would change the Fe-As-Fe bond angles and the FeAs-FeAs inter-planar distance.²¹

The occurrence of antiferromagnetic ordering of the Sm magnetic moments has been observed in specific heat experiments in polycrystalline $\text{SmFeAsO}_{1-x}\text{F}_y$.²² The Néel temperature was estimated to be $T_{\text{N}} \simeq 4.6$ K for nonsuperconducting SmFeAsO and $T_{\text{N}} \simeq 3.7$ K for superconducting $\text{SmFeAsO}_{0.85}\text{F}_{0.15}$. A similar result was found in specific heat investigations at high magnetic fields, where $T_{\text{N}} \simeq 5.4$ K for SmFeAsO and $T_{\text{N}} \simeq 3.75$ K for $\text{SmFeAsO}_{0.85}\text{F}_{0.15}$ was deduced.¹³ Additionally, the Néel temperature of SmFeAsO as derived by the specific heat appears to be almost unaffected by high fields up to 35 T.¹³ Neutron diffraction experiments on SmFeAsO reveal at low temperatures a collinear antiferromagnetic ordering of the Sm moments, in which the moments couple ferromagnetically in-plane but antiferromagnetically between adjacent planes with a magnetic moment of $\simeq 0.60(3) \mu_{\text{B}}$ per Sm ion.¹⁴ In this regard, SmFeAsO appears to exhibit a type of rare-earth antiferromagnetism which is very similar to the one observed in the layered cuprate system Sm_2CuO_4 .^{23–25} This compound was found to display a collinear magnetic-order composed of antiferromagnetically coupled Sm magnetic moments below $T_{\text{N}} \simeq 6$ K with a magnetic moment of $\simeq 0.37(3) \mu_{\text{B}}$ per Sm ion.²³ A muon-spin rotation (μSR) study in SmFeAsO reported a magnetic coupling between the Fe and the RE sublattices with an estimated moment of $\simeq 0.4 \mu_{\text{B}}$ per Sm ion.¹² Intriguingly, in the same work the magnetic structure of the Sm moments was found not only to be non-collinear to the Fe moments, but also to be non-collinear among themselves,¹² refining the picture revealed by the neutron scattering experiment.¹⁴ Interestingly, high-field electron spin resonance spectroscopy in $\text{GdFeAsO}_{1-x}\text{F}_x$ also suggest an appreciable exchange coupling between the Gd and Fe moments.²⁶

In order to study the antiferromagnetic state in $\text{SmFeAsO}_{1-x}\text{F}_y$ we performed magnetic torque, force magnetometry, and magnetoresistance measurements in single crystals in static magnetic fields up to 45 T and in pulsed fields up to 60 T at $T > 0.6$ K. The magnetic torque which initially increases with increasing field exhibits a maximum followed by a sharp reduction in fields of 35–40 T at low temperatures, and switches its sign at even higher fields. The field at which the torque is maximal displays an angular dependence, different to the one expected for an antiferromagnet in the framework of a classical spin-flop scenario. The distinct signatures of this magnetic behavior, as observed through the different experimental techniques, allow us to gain a deeper insight into the nature of the antiferromagnetic order. Furthermore, as indicated in the experiments, the low temperature antiferromagnetic state of the Sm ions persists to surprisingly high magnetic fields, well beyond the

values attained for this study.

II. EXPERIMENTAL DETAILS

Single crystals of undoped SmFeAsO (crystals A_1 , A_2 , A_3) and superconducting underdoped $\text{SmFeAsO}_{0.9}\text{F}_{0.1}$ (crystals B_1 , B_2) (all nominal compositions) with masses of a few micrograms were synthesized by the high-pressure cubic anvil technique,^{27,28} and were characterized by X-ray diffraction and by SQUID magnetometry. For the undoped SmFeAsO crystals magnetization studies reveal no traces of superconductivity, whereas for the $\text{SmFeAsO}_{0.9}\text{F}_{0.1}$ single-crystals bulk superconductivity was observed with an average $T_{\text{c}} \simeq 17$ K, by four-probe resistance measurements performed on single crystals from the same batch. Following the phase diagram published in Ref. 9 a $T_{\text{c}} \simeq 17$ K places this compound within the underdoped regime. The few reports on the antiferromagnetic phase-diagram of the Sm ions, indicate a rather weak effect of the F doping on either the Néel temperature or in the heat capacity anomaly at the transition¹¹.

Torque magnetometry of SmFeAsO and $\text{SmFeAsO}_{0.9}\text{F}_{0.1}$ single crystals at high magnetic fields was performed using static and pulsed-field facilities at the National High Magnetic Field Laboratories (NHMFL) in Tallahassee and Los Alamos, respectively. The crystals were mounted onto piezoresistive silicon micro-cantilevers (SEIKO Instruments, PRC-120 and PRC-400) and measured in a Wheatstone bridge configuration. The sensors with the mounted crystals were placed into ³He cryostats capable of achieving temperatures as low as 0.5–0.6 K. Steady magnetic fields up to 35 T were generated by a Bitter-type resistive coil and up to 45 T by a Hybrid coil-setup magnet. Pulsed magnetic fields up to 60 T were generated by a composite-material solenoid immersed in liquid nitrogen.

Low temperature magnetization measurements of antiferromagnetic SmFeAsO along the c -axis were performed with a Si based micro-electromechanical capacitive device similar to the one used in Refs. 29 and 30. At low temperatures, the sensor was calibrated by measuring the electrostatic force between the capacitive plates as a function of an external DC-bias voltage.

Four-probe magnetoresistance measurements on underdoped $\text{SmFeAsO}_{0.9}\text{F}_{0.1}$ were performed for the current flowing perpendicular to the FeAs planes in pulsed magnetic fields up to 60 T. The sample was prepared using focused ion beam techniques (FIB), with a fabrication process leading to a sample geometry which is identical to the one described in Ref. 31.

III. MAGNETIC TORQUE OF ANTIFERROMAGNETIC SYSTEMS

Antiferromagnetic compounds may show a rich variety of physics at high magnetic fields. While, at low fields the individual magnetic moments prefer to order antiferromagnetically, high magnetic fields may overcome the exchange interaction and reorient the individual magnetic moments, leading in numerous cases to a complex phase diagram with various magnetic field-induced phases. The precise knowledge of the behavior of both the magnetic torque and the magnetization of an antiferromagnetic sample, allows to investigate multiple aspects of magnetic order. Whereas magnetization gives direct information on the magnetic moment oriented along the field, the magnetic torque directly probes the anisotropy of the susceptibility in magnetically ordered or paramagnetic states. Throughout this manuscript we use the term ‘‘anisotropy’’ when referring to the intrinsic magnetic anisotropy of antiferromagnetically ordered states, given by ‘‘hard’’ and ‘‘easy’’ magnetization/susceptibility axis, or equivalently to an anisotropic susceptibility tensor.

The magnetic torque $\vec{\tau}$ of a single crystal normalized per unit of volume is defined by the vector product of the magnetization \vec{M} and the magnetic field \vec{H}

$$\vec{\tau} = \mu_0(\vec{M} \times \vec{H}). \quad (1)$$

Accordingly, the absolute value $\tau = |\vec{\tau}|$ is given by

$$\tau = \mu_0 M H \sin \varphi, \quad (2)$$

with φ the angle between \vec{M} and \vec{H} .

In the well-known case of an antiferromagnet below its Néel temperature T_N ,^{32–36} a magnetic torque τ is expected due to the magnetic anisotropy of the ordered magnetic moments. In the classical case of uniaxial magnetic anisotropy with magnetic anisotropy energy K_u , the free energy F of the system ensemble can be expressed as the sum of the magnetic and the anisotropy energies^{32,37}

$$F = -\frac{1}{2} (\chi_{\perp} \sin^2 \phi + \chi_{\parallel} \cos^2 \phi) \mu_0 H^2 - K_u \sin^2(\phi - \theta). \quad (3)$$

Here, θ describes the angle between magnetic field and the easy axis, ϕ is the angle between the magnetic field and the spin axis, and χ_{\parallel} and χ_{\perp} are the parallel and perpendicular susceptibilities with respect to the easy axis for $K_u > 0$. With these assumptions the magnetic torque at constant temperature is given by

$$\tau = -\frac{\partial F}{\partial \theta} = \frac{1}{2} (\chi_{\perp} - \chi_{\parallel}) \mu_0 H^2 \frac{\sin 2\theta}{\sqrt{\lambda^2 - 2\lambda \cos 2\theta + 1}}, \quad (4)$$

with

$$\lambda = \left(\frac{H}{H_{\text{sf}}} \right)^2, \quad (5)$$

where H_{sf} is the spin-flop field:

$$H_{\text{sf}} = \sqrt{\frac{2K_u}{\chi_{\perp} - \chi_{\parallel}}}. \quad (6)$$

Accordingly, the torque is expected to increase with increasing field up to H_{sf} where a spin reorientation occurs. In excess of this field either a gradual (flop) or discontinuous (flip) alignment of the magnetic moments along the field is expected.³⁸ In the case of a spin-flop Eq. (4) implies that for small angles $\theta \ll 45$ deg also the quantity τ/H^2 is expected to increase up to H_{sf} . In the low magnetic field limit $H \ll H_{\text{sf}}$, Eq. (4) reduces to

$$\tau = \frac{1}{2} (\chi_{\perp} - \chi_{\parallel}) \mu_0 H^2 \sin 2\theta, \quad (7)$$

and τ/H^2 results to be field independent. Additionally, one derives the field of maximum torque to depend on the angle θ as

$$H_{\text{max}}(\theta) = \frac{H_{\text{sf}}}{\sqrt{\cos(2\theta)}}. \quad (8)$$

In the case of a spin-flip, Eq. (7) is also expected to hold up to the transition at H_{sf} , where the discontinuous spin-flip occurs and the torque is reduced in excess to this field.

It would be tempting to expect a spin-flop or a spin-flip transition of the Sm-associated magnetic moments given the arrangement of moments suggested by neutron scattering experiments,¹⁴ and the conclusions reached by specific heat studies of $\text{SmFeAsO}_{1-x}\text{F}_y$ (see Ref. 13). Such a field induced spin reorientation was reported in the similar compound EuFe_2As_2 .^{39,40} However, the antiferromagnetic arrangement in $\text{SmFeAsO}_{1-x}\text{F}_y$ appears to be more complicated. Although neutron diffraction results imply a simple collinear antiferromagnetic ordering of the Sm moments,¹⁴ μSR investigations reveal evidence for an additional antiferromagnetic coupling between the Sm and the Fe magnetic moments, leading to at least three distinct configurations of the Sm moments.¹² For the latter scenario it is not obvious that the above picture of a classical antiferromagnet is sufficient to fully describe the data.

IV. EXPERIMENTAL RESULTS

The temperature dependence of the magnetic torque τ for a SmFeAsO single crystal was measured in various magnetic fields up to 35 T with a fixed angle $\theta \sim 1^\circ$ and is presented in Fig. 1a. Below ~ 5 K a drastic increase in $\tau(T)$ is observed, due to the occurrence of antiferromagnetic order. This is more clearly exposed in Fig. 1b, where the quantity τ/H^2 is plotted as a function of T . All curves show a linear dependence in temperature below a characteristic temperature $T_{\text{onset}}(H)$. Notice that $T_{\text{onset}}(H)$ decreases with increasing magnetic field. The nearly linear dependence of τ/H^2 (see Fig. 1b) at low

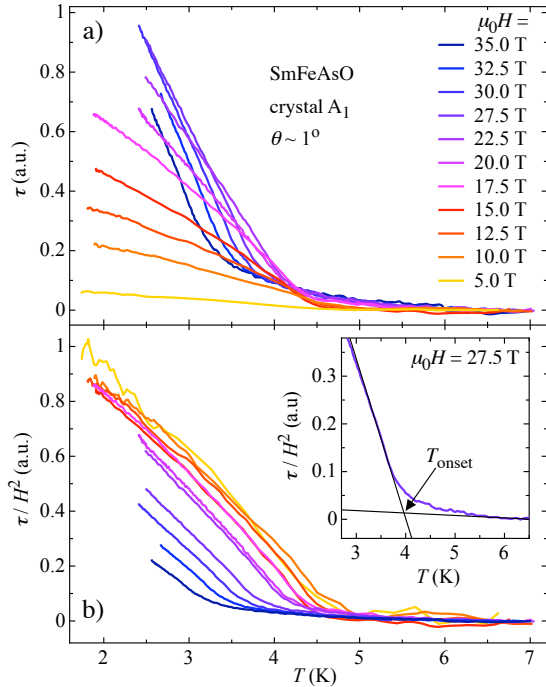


FIG. 1: (color online) Magnetic torque τ for a SmFeAsO single crystal in the vicinity of the onset of the antiferromagnetic state for fields nearly along the c -axis of the crystal. a) Measured $\tau(T)$ at different magnetic fields H for the SmFeAsO crystal A₁, where the angle between H and the c -axis is fixed at $\theta \sim 1^\circ$. b) τ/H^2 as a function of T . All branches follow a linear behavior below $T_{\text{onset}}(H)$, typical for an antiferromagnetic state. The inset shows $\tau(T)/H^2$ at $\mu_0 H = 27.5$ T. The temperature T_{onset} is defined by the crossing of the linearly extrapolated data from the high and low temperature regimes, respectively.

temperatures is typical for an antiferromagnetic state according to Eq. (4), assuming χ_\perp to be temperature independent and χ_\parallel to scale linearly with $T < T_N$ (see *e.g.* Ref. 38). The inset to Fig. 1b shows τ/H^2 measured at $\mu_0 H = 27.5$ T, demonstrating how $T_{\text{onset}}(H)$ is extracted from the data (by analyzing the crossing of two straight lines obtained by extrapolating the low and the high temperature behavior of τ/H^2).

Figure 2a shows the magnetic field dependence of the torque signal $\tau(H)$ for a SmFeAsO single crystal in the temperature range $T \leq 5$ K, measured at a fixed angle $\theta \sim 1^\circ$. Whereas at $T \sim 5$ K essentially no torque signal is observed, $\tau(H)$ increases strongly with decreasing temperature. At very low magnetic fields, the magnetic torque in the antiferromagnetic state is expected to be almost zero, since here $\tau(H)$ is proportional to H^2 . However, the data presented in Fig. 2a, indicate an additional contribution to the torque at low fields, possibly due to a change in the antiferromagnetic anisotropy at low magnetic fields, or some small additional anisotropic magnetic contributions to the torque. Above $\mu_0 H \sim 5$ T, $\tau(H)$ increases almost quadratically with H towards a

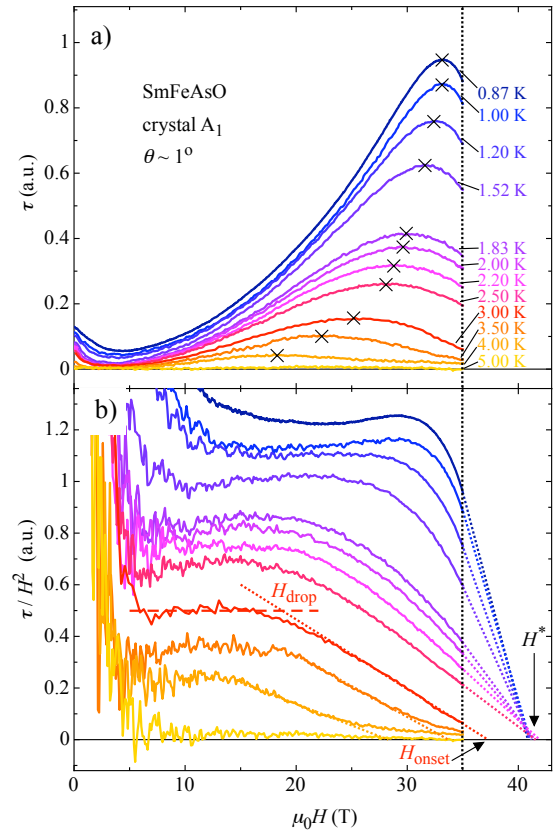


FIG. 2: (color online) High-field behavior of the magnetic torque in antiferromagnetic SmFeAsO. a) Magnetic torque $\tau(H)$ at different temperatures for the SmFeAsO crystal A₁, where the angle between H and the c -axis is fixed to $\theta \sim 1^\circ$. The maximum in torque at the field H_{max} is marked by the crosses and is temperature dependent. b) τ/H^2 as a function of H . All curves are almost field independent in the intermediate field range 10–20 T. For temperatures $T \geq 3$ K the dotted lines above fields exceeding 35 T are extrapolations to estimate $H_{\text{onset}}(T)$, where $\tau(H)/H^2$ is expected to reach zero. Below $T \leq 2.5$ K, all these extrapolations point to the same field $\mu_0 H^* \approx 40$ T. $H_{\text{drop}}(T)$ denotes the field where τ/H^2 starts being suppressed. The convention for H_{drop} and H_{onset} is shown for the $T = 3$ K data.

field dependent maximum beyond which it exhibits a pronounced decrease, indicating a change in the original spin arrangement at very high fields. We define the magnetic field where the maximum in $\tau(H)$ is observed as the field $H_{\text{max}}(T)$ which is indicated by crosses in Fig. 2a. In Fig. 2b the quantity τ/H^2 is plotted as a function of H . At intermediate field strengths, τ/H^2 is essentially constant as a function of H , whereas at low magnetic fields, the previously discussed additional contribution dominates τ/H^2 which tends to diverge as the field is ramped down to zero. Above H_{drop} the quantity τ/H^2 decreases rapidly with increasing H . The linearly extrapolated data, as shown by the dotted lines in Fig. 2b, leads to an estimate of the magnetic field where τ becomes zero. Down to 3 K these fields are found to

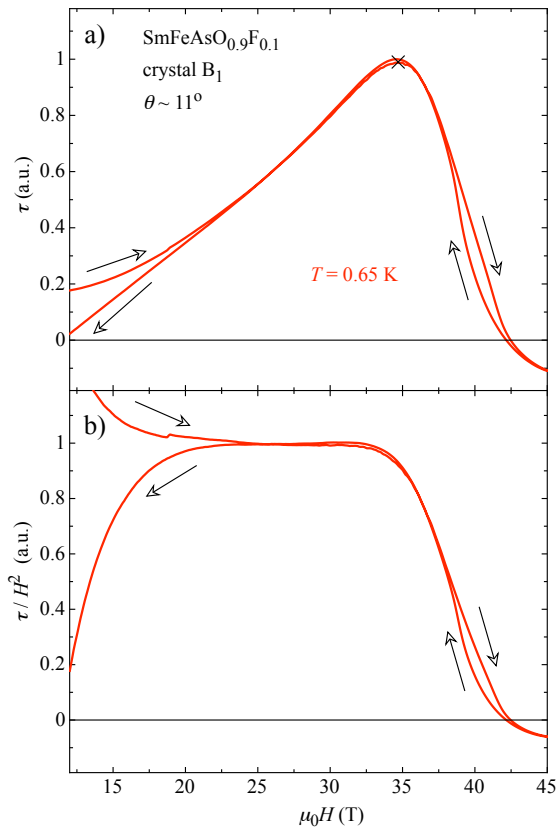


FIG. 3: (color online) Magnetic torque τ as a function of H for a superconducting $\text{SmFeAsO}_{0.9}\text{F}_{0.1}$ single crystal. a) τ for crystal B_1 ($T_c \simeq 17$ K) at a fixed angle $\theta \simeq 11^\circ$ and at 0.65 K. The torque maximum is marked by a cross. A hysteresis is observed above the maximum in $\tau(H)$. b) τ/H^2 as a function of H .

be strongly temperature dependent and are denoted as $H_{\text{onset}}(T)$, whereas the estimated fields for $T \leq 2.5$ K are almost constant and are labeled as $H^*(T)$. Clearly H_{onset} scales with the value of T_{onset} as defined in Fig. 1b.

The data presented in Figs. 1 and 2 suggest the occurrence of a metamagnetic transition in SmFeAsO which might correspond to either an onset of a gradual spin-orientation or a discontinuous spin-canting transition at the field H_{max} . Throughout this manuscript we define the term “metamagnetism” simply as a superlinear increase in the magnetization under a given external field⁴¹. As this anomaly in magnetic torque is detected in the range of temperatures where the antiferromagnetism of Sm-ions is present, one might expect a similar transition for superconducting $\text{SmFeAsO}_{0.9}\text{F}_{0.1}$ single crystals. Notice that the Sm-associated antiferromagnetic order was observed in superconducting $\text{SmFeAsO}_{1-x}\text{F}_y$ samples.¹³ In Fig. 3a we show $\tau(H)$ for the superconducting $\text{SmFeAsO}_{0.9}\text{F}_{0.1}$ single crystal B_1 at 0.65 K and at an angle $\theta \sim 11^\circ$, acquired by increasing and decreasing the external magnetic field from $\mu_0 H = 11.5$ T to 45 T, respectively. Both, increasing and decreasing field

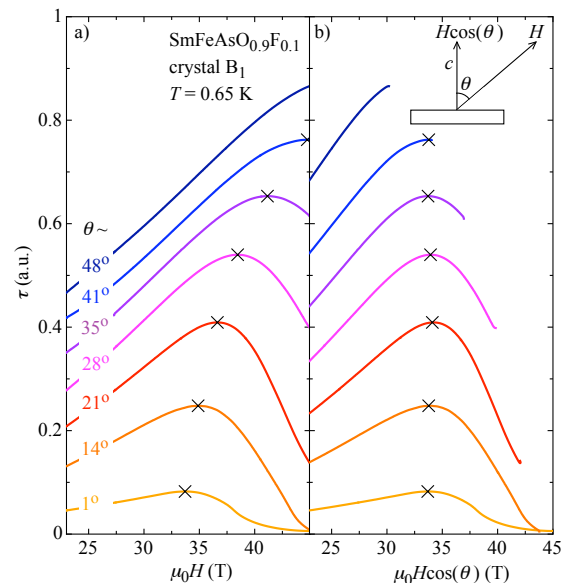


FIG. 4: (color online) Magnetic torque $\tau(H)$ as a function of the magnetic field H and for various angles θ between H and c -axis of the superconducting $\text{SmFeAsO}_{0.9}\text{F}_{0.1}$ single crystal B_1 ($T_c \simeq 17$ K). The maxima shift with θ according to $H/\cos(\theta)$ (panel a) or, equivalently, occur at the same c -component $H \cos(\theta) \simeq 34$ T perpendicular to the planes (panel b). Hence, the position of the torque maximum observed at high fields is related to a magnetization component in the ab -plane.

branches of $\tau(H)$ are displayed in order to visualize the irreversible response characteristic of the superconducting state below the irreversibility field H_{irr} and hysteretic behavior observed for fields beyond H_{max} . For this sample with a rather low $T_c \simeq 17$ K, we do not expect H_{irr} to be located above $\simeq 23$ T, even at 0.6 K, as indicated by the low field irreversible branches in Fig. 3a. Hence, the irreversible torque signal above H_{max} is not related to superconductivity, but to the antiferromagnetic state of the Sm magnetic moments. The data suggests that the torque would display negative values for fields exceeding a certain value H^* . In Fig. 3b we present the same data set but as $\tau(H)/H^2$ as a function of H which displays very similar qualitative behavior with respect to the traces presented in Fig. 2b. By comparing Figs. 2a and 3a, one notices that the maximum in the torque signal at low temperatures occurs at a slightly higher magnetic field $H_{\text{max}} \simeq 35$ T for the superconducting crystal B_1 than the one for the nonsuperconducting SmFeAsO crystal A_1 with $H_{\text{max}} \simeq 33$ T. However, the data of each sample were recorded at different angles θ . Hence, in order to compare the data presented in Figs. 2 and 3, we investigated the angular dependence of H_{max} in the $\text{SmFeAsO}_{0.9}\text{F}_{0.1}$ crystal B_1 . Figure 4a shows the magnetic torque $\tau(H)$ for various angles θ . The maxima in $\tau(H)$ are clearly shifting to higher fields with increasing θ . Figure 4b shows τ as a function of the rescaled

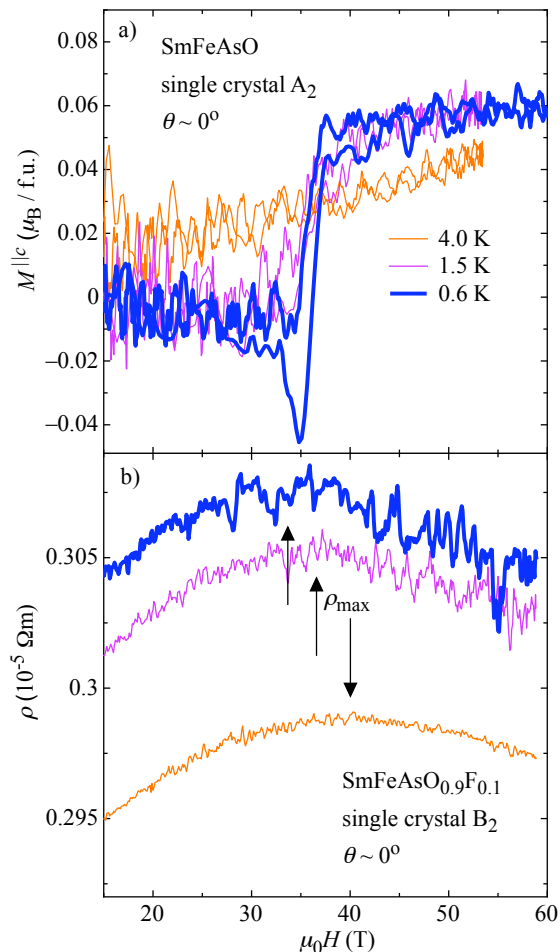


FIG. 5: (color online) Experimental indication for a rearrangement of the c -axis component of the magnetization at high fields. a) Magnetization measured with the field perpendicular to the planes in a force magnetometer for the SmFeAsO crystal A₂ at $T \simeq 0.6$ K, $\simeq 1.5$ K, and $\simeq 4$ K, respectively. At the temperature $T \simeq 0.6$ K the magnetization jumps by $M_{\text{jump}} \simeq 0.06(2) \mu_{\text{B}}$ per formula unit (f.u.) at ~ 35 T. b) Magnetoresistance $\rho(H)$ of the SmFeAsO_{0.9}F_{0.1} crystal B₂ in pulsed magnetic fields perpendicular to the planes. The magnetoresistance shows a maximum ρ_{max} between 35 – 40 T, which shifts to higher fields with increasing temperatures (indicated by the arrows).

magnetic field

$$H^{\parallel c} = H \cos(\theta). \quad (9)$$

All torque maxima in $\tau(H^{\parallel c})$ are observed at essentially the same c -axis component of the magnetic field. This would suggest that the maximum of torque is associated with a reorientation or canting of a magnetization component in the conducting planes.

Obviously, the observed angular dependence of the torque maxima is different from that expected for a classical anisotropic antiferromagnet [see Eq (8)]. However, both SmFeAsO and SmFeAsO_{1-x}F_y exhibit a similar response in the torque concerning the rearrangement of the

low-temperature antiferromagnetic order in fields up to ~ 35 T, and show a clear drop in $\tau(H)$ above $H_{\text{max}}(T)$. Clearly, only the c -axis component of the magnetic field is responsible for this distinct feature in the torque signal.

We extracted the absolute value of the change in the c -axis component of the magnetic moment m_z at H_{max} by performing magnetic force measurements at low temperatures. The mass of the crystal A₂ which was selected from the same batch of SmFeAsO investigated above, was determined by monitoring the shift in the resonance frequency of the device and was found to be equal to $\simeq 2.1(6) \mu\text{g}$. The sensor with the mounted sample was placed slightly off field center, in order to make use of the magnetic field gradient $\partial H/\partial z$ of the solenoid. The value of $\partial H_z/\partial z$ was estimated by analyzing the geometry of the solenoid. The magnetization along the c -axis is then derived accordingly

$$M_z = \frac{F_z}{\mu_0 V} \left(\frac{\partial H_z}{\partial z} \right)^{-1}. \quad (10)$$

The change in magnetization at H_{max} is found by extracting the magnetic moment from magnetic force measurements performed as a function of the field applied along the c -axis. Figure 5a presents the calibrated magnetization data obtained at various temperatures. As clearly seen, the magnetization shows a sharp jump at $\simeq 35$ T at $T = 0.6$ K (θ is kept at nearly zero degrees during these measurements) saturating at a value of only $\sim 0.06(2) \mu_{\text{B}}$ per formula unit (f.u.). This value is rather small, when compared to the estimates for the full Sm magnetic moment of $\simeq 0.4 - 0.6 \mu_{\text{B}}$ reported in the literature,^{12,14} suggesting that only a partial reorientation of the magnetic moments is observed at $H_{\text{max}} \simeq 35$ T. These results indicate that much higher fields are required to fully suppress the antiferromagnetic order. Notice that no additional jumps in the c -axis component of the magnetization are observed at base temperature and under fields up to 60 T, see Fig. 5a.

We have also studied the magnetoresistance $\rho(H)$ of the underdoped SmFeAsO_{0.9}F_{0.1} crystal B₂ for electric currents flowing perpendicularly to the FeAs-planes in pulsed magnetic fields up to 60 T. These experiments provide additional evidence for the observed magnetic rearrangement (see Fig. 5b). At fields below 35 – 40 T, a positive magnetoresistance was observed, while the material shows negative magnetoresistance at higher fields. In our scenario, the negative magnetoresistance is indicative of a reduction of spin scattering as the Sm ions undergo a spin reorientation transition. The maximum observed in the $\rho(H)$ curves shifts to higher fields with increasing temperature. At low temperatures, the field where the maximum ρ_{max} in the resistivity is observed, coincides with the field where the jump in magnetization occurs.

In order to further characterize this high-field metamagnetic behavior associated with the Sm-antiferromagnetic order, we performed additional torque measurements in pulsed magnetic fields up to 60 T for the

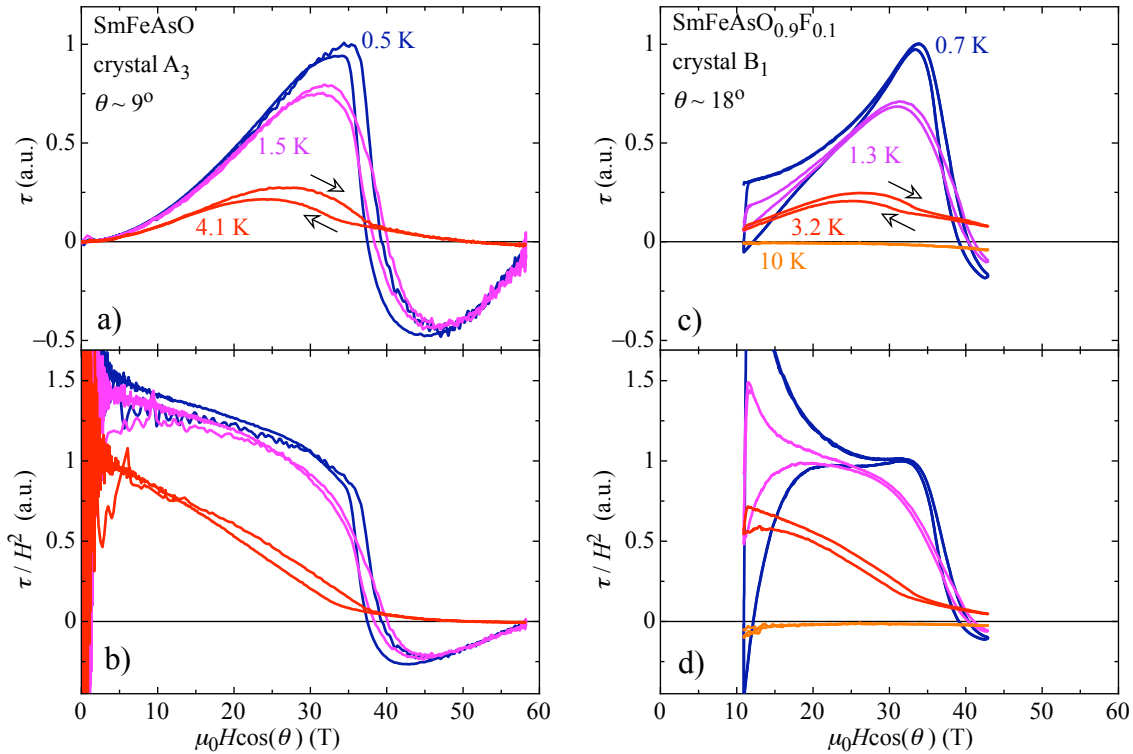


FIG. 6: (color online) Magnetic torque for single crystalline SmFeAsO and SmFeAsO_{0.9}F_{0.1}. For a comparison with measurements performed at different angles θ (see Figs. 2, 3, and 4) the field is given as $H \cos(\theta)$. a) $\tau(H)$ for the SmFeAsO crystal A₃ measured at a fixed angle $\theta \sim 9^\circ$. b) τ/H^2 obtained from the data shown in panel a). c) and d) the same as in a) and b) but for the SmFeAsO_{0.9}F_{0.1} single crystal B₁.

SmFeAsO crystal A₃. Figure 6a displays $\tau(H)$ recorded at various temperatures and at a fixed angle $\theta \sim 9^\circ$. At fields below 35 – 40 T the qualitative behavior of $\tau(H)$ strongly resembles the data shown in Fig. 2a. It is found that for $H > H^*$ the magnetic torque indeed becomes negative. It is interesting to note that a change of sign in magnetic torque could also be related to a change of easy axis in magnetic ordering. A similar effect was reported for molecular magnets.⁴² In Fig. 6b $\tau(H)/H^2$ is presented. The c -axis components of the fields H_{\max} and H^* as observed in Figs. 6a and 6b are in terms of $\tau(H \cos(\theta))$ in good agreement to those determined in Figs. 2a and 2b. Figures 6c and 6d show magnetic torque data obtained for the SmFeAsO_{0.9}F_{0.1} crystal B₁ probed by static magnetic field. Obviously, the magnetic torque for both, superconducting and non-superconducting samples exhibit the same qualitative behavior in field.

Reviewing the overall experimental data for undoped SmFeAsO presented in Figs. 1, 2, 5, and 6 one concludes that the original antiferromagnetic arrangement of the Sm-magnetic moments persists to high magnetic fields of the order of 35 T. Although T_N is only about 5 K, it is remarkable that an energy scale of 35 T is required to perturb this antiferromagnetic ground state. This scenario can be explained by invoking a difference in the energies

corresponding to the ordering temperature T_N and the spin-flop field H_{sf} , resulting from a reduced dimensionality in the magnetic interactions. In this picture the magnetic exchange constants, characterized most likely by an in-plane exchange constant J and a much smaller out of the plane one J_\perp , could be very anisotropic, similar to the situation in Ref. 43. A phase-transition takes place, when all moments become coherently coupled below $k_B T_N \propto J_\perp \ll J$. However, the metamagnetic transition, or the field-induced rearrangement of an anisotropic antiferromagnetic configuration of localized moments as observed here, would involve all the relevant energy scales leading to such a configuration, in particular the largest J , thus explaining the large value of the saturation field $H_{\text{sf}} \propto J \gg J_\perp$. As for undoped SmFeAsO more than two anisotropic exchange energies might be involved in the antiferromagnetic order, as we may infer from results of earlier investigations.^{12,13}

In Fig. 7 a color map of $\tau(H)/H^2$ as a function of $\mu_0 H \cos(\theta)$ and T , based on the results for SmFeAsO, is presented. The experimental data shown in Fig. 6b have been combined in order to generate a map, illustrating $\tau(H)/H^2$ in a normalized scale as a function of temperature and field. For completeness our estimates of the quantities H_{\max} , H_{drop} , H^* , H_{onset} , T_{onset} , M_{jump} , and ρ_{\max} of Figs. 1, 2, and 5 are shown as well. Interestingly,

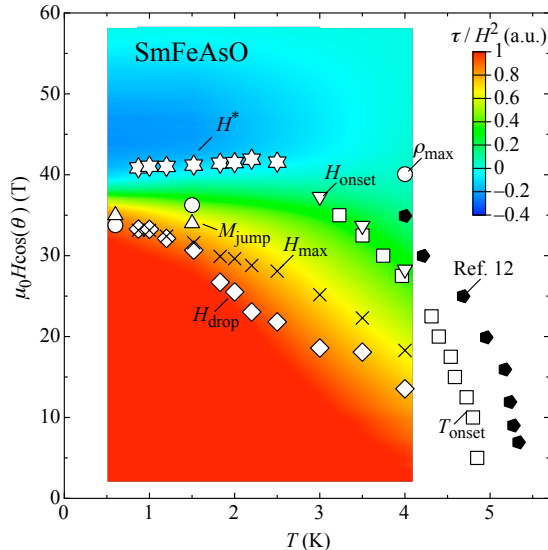


FIG. 7: (color online) $H-T$ phase-diagram of SmFeAsO from magnetic torque τ , magnetization M , and magnetoresistivity ρ measurements. At low temperatures, the application of high magnetic fields in the order of 35 to 40 T, disturbs the original antiferromagnetic state of the Sm-ions resulting in an antiferromagnetic rearrangement in fields exceeding H_{\max} . For the sake of comparison, we include the phase-diagram obtained from specific heat measurements in polycrystalline samples (having a higher Néel temperature $T_N \simeq 5.4$ K).¹³ The different symbols depict the field and temperature dependence of various physical quantities defined in previous figures and within the text.

the region where the change of the sign of the torque is observed, appears to be almost temperature independent.

V. DISCUSSION AND SUMMARY

In summary in this work, we present evidence for a metamagnetic anomaly occurring in magnetic fields in the order of 35 – 40 T in both SmFeAsO and SmFeAsO_{0.9}F_{0.1} single crystals. At first glance, it would seem that this transition corresponds to the suppression of the antiferromagnetic order of the Sm-ions. However, we found the change of the saturation moment at the transition [$\simeq 0.06(2)$ μ_B] to be much smaller than the value for the full Sm-moments of $\simeq 0.4 - 0.6$ μ_B extracted by μ SR and neutron diffraction.^{12,14} Hence, although the observed anomaly in the torque in magnetic fields between $H_{\max}(T)$ and $H_{\text{drop}}(T)$ is obviously related to a spin-canting, evidenced by the similarity of the presented data to the expectations for a spin-flop or a spin-flip, it apparently involves a partial spin reorientation only. This scenario appears to be in agreement to the μ SR result of SmFeAsO, which suggests a rather complex magnetic structure of the sublattice of Sm mag-

netic moments, where the spins are not expected to align collinearly. Our results indicate that extended high magnetic fields investigations in SmFeAsO are required to reach the full polarization of the magnetic moments at low temperatures. It remains to be answered in which manner antiferromagnetism in SmFeAsO_{1-x}F_y is suppressed in even higher fields. It is possible that the spin density wave state formed due to the Fe magnetic moments is crucial for this high magnetic field behavior.

We show evidence for the existence of a rearrangement of antiferromagnetic ordering in the SmFeAsO_{1-x}F_y series, which is undoubtedly associated with the Néel state of the Sm-moments and their coupling to the Fe sublattice. Extremely high magnetic fields are necessary to induce it, despite the relatively low value of the Néel temperature, indicating that this antiferromagnetic state is highly anisotropic, *i.e.* quasi-two-dimensional. The very low value of the recovered saturation moment suggests that a new antiferromagnetic state is induced by high magnetic fields with partially reoriented or canted magnetic moments. A full suppression of Sm antiferromagnetism would require enormous magnetic fields which are beyond the field range of this study.

It might be worthwhile to further investigate under high magnetic fields the detailed magnetic and superconducting phase diagram of the various REFeAsO_{1-x}F_y systems, in order to elucidate in greater detail the role of the interaction between the magnetic moment of the rare-earth ion and the electrons mainly responsible for the superconducting state. An obvious route would be to fully explore the upper critical field $H_{c2}(T)$, which, due to its large value, is only partially accessible to the present study. Apparently, there might be some differences in the temperature evolution of H_{c2} between the SmFeAsO_{1-x}F_y (Refs. 28 and 31) and the NdFeAsO_{1-x}F_y (Ref. 44) compounds. Only further studies, perhaps not based solely on dissipative transport measurements, can clarify the origin of such differences.

Finally, and although the incorporation of magnetic rare-earth elements in the SmFeAsO_{1-x}F_y system increases the superconducting transition temperature considerably, our observations suggest that its magnetism may be detrimental for superconductivity at very high magnetic fields. The clarification of this point is particularly relevant for these materials, since the combination of extremely high upper critical fields,^{31,44} large and isotropic critical currents,^{27,28,31,45} and unconventional magnetic anisotropy,^{46,47} make them potentially relevant for technological applications.

VI. ACKNOWLEDGEMENTS

The authors acknowledge stimulating discussions to A. Gurevich and F. Mila. The NHMFL is supported by NSF through NSF-DMR-0084173 and the State of Florida. L. B. is supported by DOE-BES through

award DE-SC0002613. K. N., H. B. C., and L. B. are supported by the NHMFL-UCGP program. This work was also partially supported by the Swiss National Science Foundation, the NCCR program MaNEP,

and the Polish Ministry of Science and Higher Education, within the research project for the years 2007-2010 (No. N N202 4132 33).

-
- * Electronic address: balicas@magnet.fsu.edu
- ¹ J. G. Bednorz and K. A. Müller, *Z. Phys. B: Condens. Matter* **64**, 189 (1986).
 - ² Y. Kamihara, T. Wanabe, M. Hirano, and H. Hosono, *J. Am. Chem. Soc.* **130**, 3296 (2008).
 - ³ Z.-A. Ren, W. Lu, J. Yang, W. Yi, X. L. Shen, Z. C. Li, G. C. Che, X. L. Dong, L. L. Sun, F. Zhou, and Z.-X. Zhao, *Chin. Phys. Lett.* **25**, 2215 (2008).
 - ⁴ R. H. Liu, G. Wu, T. Wu, D. F. Fang, H. Chen, S. Y. Li, K. Liu, Y. L. Xie, X. F. Wang, R. L. Yang, L. Ding, C. He, D. L. Feng, and X. H. Chen, *Phys. Rev. Lett.* **101**, 087001 (2008).
 - ⁵ I. I. Mazin, D. J. Singh, M. D. Johannes, and M. H. Du, *Phys. Rev. Lett.* **101**, 057003 (2008).
 - ⁶ C. de la Cruz, Q. Huang, J. W. Lynn, J. Y. Li, W. Ratcliff, J. L. Zarestky, H. A. Mook, G. F. Chen, J. L. Luo, N. L. Wang, and P. C. Dai, *Nature* **453**, 899 (2008).
 - ⁷ D. J. Singh and M.-H. Du, *Phys. Rev. Lett.* **100**, 237003 (2008).
 - ⁸ A. I. Coldea, J. D. Fletcher, A. Carrington, J. G. Analytis, A. F. Bangura, J.-H. Chu, A. S. Erickson, I. R. Fisher, N. E. Hussey, and R. D. McDonald, *Phys. Rev. Lett.* **101**, 216402 (2008).
 - ⁹ A. J. Drew, C. Niedermayer, P. J. Baker, F. L. Pratt, S. J. Blundell, T. Lancaster, R. H. Liu, G. Wu, X. H. Chen, I. Watanabe, V. K. Malik, A. Dubroka, M. Rössle, K. W. Kim, C. Baines, and C. Bernhard, *Nature Materials* **8**, 310 (2009).
 - ¹⁰ J. Zhao, Q. Huang, C. de la Cruz, S. Li, J. W. Lynn, Y. Chen, M. A. Green, G. F. Chen, G. Li, Z. Li, J. L. Luo, N. L. Wang, and P. C. Dai, *Nature Materials* **7**, 953 (2008).
 - ¹¹ L. Ding, C. He, J. K. Dong, T. Wu, R. H. Liu, X. H. Chen, and S. Y. Li, *Phys. Rev. B* **77**, 180510(R) (2008); Y. Kamihara, T. Nomura, M. Hirano, J. E. Kim, K. Kato, M. Takata, Y. Kobayashi, S. Kitao, S. Higashitaniguchi, Y. Yoda, *New J. Phys.* **12**, 033005 (2010).
 - ¹² H. Maeter, H. Luetkens, Y. G. Pashkevich, A. Kwadrin, R. Khasanov, A. Amato, A. A. Gusev, K. V. Lamsonova, D. A. Chervinskii, R. Klingeler, C. Hess, G. Behr, B. Büchner, and H.-H. Klauss, *Phys. Rev. B* **80**, 094524 (2009).
 - ¹³ S. C. Riggs, C. Tarantini, J. Jaroszynski, A. Gurevich, A. Palenzona, M. Putti, T. Duc Nguyen, and M. Affronte, *Phys. Rev. B* **80**, 214404 (2009).
 - ¹⁴ D. H. Ryan, J. M. Cadogan, C. Ritter, F. Canepa, A. Palenzano, and M. Putti, *Phys. Rev. B* **80**, 220503(R) (2009).
 - ¹⁵ Y. Qiu, W. Bao, Q. Huang, T. Yildirim, J. M. Simmons, M. A. Green, J. W. Lynn, Y. C. Gasparovic, J. Li, T. Wu, G. Wu, and X. H. Chen, *Phys. Rev. Lett.* **101**, 257002 (2008).
 - ¹⁶ C. Tarantini, A. Gurevich, D. C. Larbalestier, Z.-A. Ren, X.-L. Dong, W. Lu, and Z.-X. Zhao, *Phys. Rev. B* **78**, 184501 (2008).
 - ¹⁷ S. A. J. Kimber, D. N. Argyriou, F. Yokaichiya, K. Habicht, S. Gerischer, T. Hansen, T. Chatterji, R. Klingeler, C. Hess, G. Behr, A. Kondrat, and B. Büchner, *Phys. Rev. B* **78**, 140503(R) (2008).
 - ¹⁸ W. Tian, W. Ratcliff, M. G. Kim, J.-Q. Yan, P. A. Kienzle, Q. Huang, B. Jensen, K. W. Dennis, R. W. McCallum, T. A. Lograsso, R. J. McQueeney, A. I. Goldman, J. W. Lynn, and A. Kreyssig, *Phys. Rev. B* **82**, 060514(R) (2010).
 - ¹⁹ N. D. Ashcroft and M. D. Mermin, *Solid State Physics* Saunders College Publishing (1976).
 - ²⁰ H. Kontani and S. Onari, *Phys. Rev. Lett.* **104**, 157001 (2010).
 - ²¹ V. Vildosola, L. Pourovskii, R. Arita, S. Biermann, and A. Georges, *Phys. Rev. B* **78**, 064518 (2008).
 - ²² L. Ding, C. He, J. K. Dong, T. Wu, R. H. Liu, X. H. Chen, and S. Y. Li, *Phys. Rev. B* **77**, 180510(R) (2008).
 - ²³ I. W. Sumarlin, S. Skanthakumar, J. W. Lynn, J. L. Peng, Z. Y. Li, W. Jiang, and R. L. Greene, *Phys. Rev. Lett.* **68**, 2228 (1992).
 - ²⁴ R. Sachidnandam, T. Yildirim, A. B. Harris, A. Aharony, and O. Entin-Wohlman, *Phys. Rev. B* **56**, 260 (1997).
 - ²⁵ T. Strach, T. Ruf, M. Cardona, C. T. Lin, S. Jandl, V. Nekvasil, D. I. Zhigadlo, S. N. Barilo, and S. V. Shiryayev, *Phys. Rev. B* **56**, 5578 (1997).
 - ²⁶ A. Alfonsov, F. Murányi, V. Kataev, G. Lang, N. Leps, L. Wang, R. Klingeler, A. Kondrat, C. Hess, S. Wurmehl, A. Köhler, G. Behr, S. Hempel, M. Deutschmann, S. Katrych, N. D. Zhigadlo, Z. Bukowski, J. Karpinski, and B. Büchner, arXiv:cond-mat/1010.5070v1 (unpublished).
 - ²⁷ N. D. Zhigadlo, S. Katrych, Z. Bukowski, S. Weyeneth, R. Puzniak, and J. Karpinski, *J. Phys.: Condens. Matter* **20**, 342202 (2008).
 - ²⁸ J. Karpinski, N. D. Zhigadlo, S. Katrych, Z. Bukowski, P. Moll, S. Weyeneth, H. Keller, R. Puzniak, M. Tortello, D. Daghero, R. Gonnelli, I. Maggio-Aprile, Y. Fasano, O. Fischer, K. Rogacki, and B. Batlogg, *Physica C* **469**, 370 (2009).
 - ²⁹ V. Aksyuk, F. F. Balakirev, G. S. Boebinger, P. L. Gammel, R. C. Haddon, and D. J. Bishop, *Science* **280**, 720 (1998).
 - ³⁰ C. A. Bolle, V. Aksyuk, F. Pardo, P. L. Gammel, E. Zeldov, E. Bücher, R. Boie, D. J. Bishop, and D. R. Nelson, *Nature* **399**, 43 (1999).
 - ³¹ P. J. W. Moll, R. Puzniak, F. Balakirev, K. Rogacki, J. Karpinski, N. D. Zhigadlo, and B. Batlogg, *Nature Materials* **10**, 628 (2010).
 - ³² K. Yosida, *Prog. Theor. Phys.* **6**, 691 (1951).
 - ³³ H. Tanaka, S. Hara, M. Tokumoto, N.-B. Cui, H. Kobayashi, and A. Kobayashi, *J. Low Temp. Phys.* **142**, 609 (2006).
 - ³⁴ X.-Y. Wang, L. Wang, Z.-M. Wang, G. Su, and S. Gao, *Chem. Matter* **17**, 6369 (2005).
 - ³⁵ M. Tokumoto, H. Tanaka, T. Otsuka, H. Kobayashi, and A. Kobayashi, *Polyhedron* **24**, 2793 (2005).
 - ³⁶ T. Kawamoto, Y. Bando, T. Mori, T. Konoike,

- Y. Takahide, T. Terashima, S. Uji, K. Takahiya, and T. Otsubo, *Phys. Rev. B* **77**, 224506 (2008).
- ³⁷ H. Uozaki, T. Sasaki, S. Endo, and N. Toyota, *J. Phys. Soc. Jap.* **69**, 2759 (2000).
- ³⁸ S. Blundell, *Magnetism in Condensed Matter* Oxford University Press (2001).
- ³⁹ S. Jiang, Y. Luo, Z.-A. Ren, Z. Zhu, C. Wang, X. Xu, Q. Tao, G. Cao, and Z. Xu, *New J. Phys.* **11**, 025007 (2009).
- ⁴⁰ Y. Xiao, Y. Su, W. Schmidt, K. Schmalzl, C. M. N. Kumar, S. Price, T. Chatterji, R. Mittal, L. J. Chang, S. Nandi, N. Kumar, S. K. Dhar, A. Thamizhavel, and T. Brueckel, *Phys. Rev. B* **81**, 220406(R) (2010).
- ⁴¹ R. S. Perry, L. M. Galvin, S. A. Grigera, L. Capogna, A. J. Schofield, A. P. Mackenzie, M. Chiao, S. R. Julian, S. I. Ikeda, S. Nakatsuji, Y. Maeno, and C. Pfleiderer, *Phys. Rev. Lett.* **86**, 2661 (2001).
- ⁴² O. Waldmann, L. Zhao, and L. K. Thompson, *Phys. Rev. Lett.* **88**, 066401 (2002).
- ⁴³ P. A. Goddard, J. Singleton, P. Sengupta, R. D. McDonald, T. Lancaster, S. J. Blundell, F. L. Pratt, S. Cox, N. Harrison, J. L. Manson, H. I. Southerland, and J. A. Schlueter, *New J. Phys.* **10**, 083025 (2008).
- ⁴⁴ J. Jaroszynski, F. Hunte, L. Balicas, Y.-J. Jo, I. Raicevic, A. Gurevich, D. C. Larbalestier, F. F. Balakirev, L. Fang, P. Cheng, Y. Jia, and H.-H. Wen, *Phys. Rev. B* **78**, 174523 (2008).
- ⁴⁵ N. D. Zhigadlo, S. Katrych, S. Weyeneth, R. Puzniak, P. Moll, Z. Bukowski, J. Karpinski, H. Keller, and B. Batlogg, *Phys. Rev. B* **82**, 064517 (2010).
- ⁴⁶ S. Weyeneth, R. Puzniak, U. Mosele, N. D. Zhigadlo, S. Katrych, Z. Bukowski, J. Karpinski, S. Kohout, J. Roos, and H. Keller, *J. Supercond. Nov. Magn.* **22**, 325 (2009).
- ⁴⁷ S. Weyeneth, R. Puzniak, N. D. Zhigadlo, S. Katrych, Z. Bukowski, J. Karpinski, and H. Keller, *J. Supercond. Nov. Magn.* **22**, 347 (2009).